Available online at www.sciencedirect.com
ScienceDirect
Cement and Concrete Research 37 (2007) 725–734
Cement and Concrete Research

Time-dependent response of ECC: Characterisation of creep and rate dependence

William P. Boshoff *, Gideon P.A.G. van Zijl

Division for Structural Engineering, University of Stellenbosch, Private Bag X1, Stellenbosch, South Africa

Received 15 November 2005; accepted 6 February 2007

1. Introduction

The mechanical behaviour of cement-based material is highly time-dependent and rate-dependent not only for dynamic cases, but also in the quasi-static loading range, where inertia and wave effects are negligible [1–5]. Creep is a well-known phenomenon in terms of continued deformation under sustained load. Less well-known is the reduced strength of a cement-based material with a reduction in the loading rate [3,6]. An example is given in Fig. 1(a), which shows the dependence of peak resistance of notched concrete beams on the deflection rate in three point bending [3]. An approximate 45% increase in peak resistance was the result of an increase in the deflection rate from 0.05 μm/s (peak load after about 80 min) to 50 μm/s (peak load after about 5 s).

By the same mechanisms causing such reduction in resistance with loading rate decrease, delayed failure may occur in structures loaded at levels below the "static" peak resistance, as is evident from Fig. 1(b) for uni-axial tensile creep experiments [7]. The time to failure varies from a few seconds at a high sustained load level of 90% of the peak load, to several hours at 65% to 75% of the peak load.

The most prominent micromechanical mechanisms of the time dependence are moisture migration at a low to medium load and micro-cracking at a high load. Heterogeneities in the microstructure cause stress peaks, which may exceed inter-particular bond and has this micro-cracking as a result. In tension, the effect of the micro-cracking is worsened and will cause a sudden and brittle failure if the material is not reinforced [8].

Many phenomological models have been created and verified to simulate the rate-dependant behaviour of cement-based materials, e.g. [6,9,10]. Mihashi and Wittmann [6] created a model that is based on a power law to describe the increase of strength with an increase of the loading rate. The model was calibrated for bending and compression.

Although the mechanisms that cause the time-dependant behaviour are intertwined on the micro-level, a phenomological

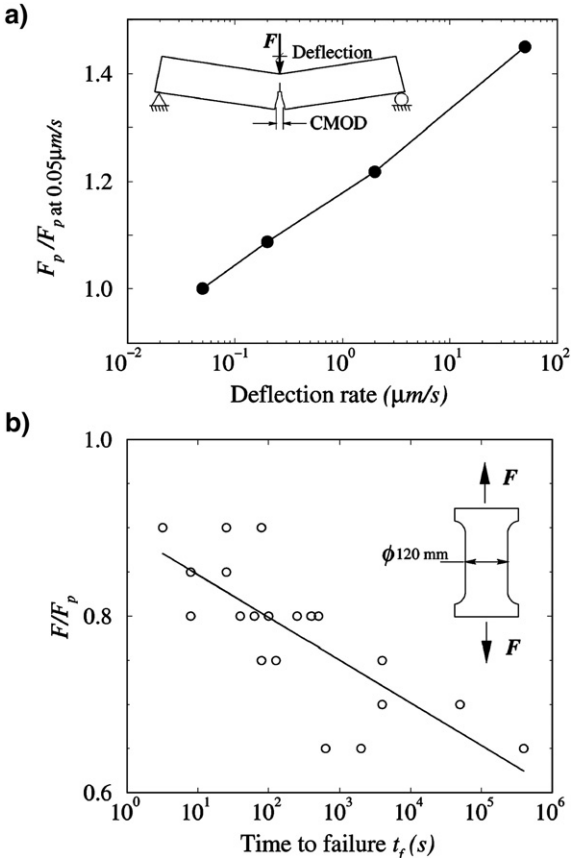

Fig. 1. a) Concrete rate-dependant strength increase in quasi-static loading range [3]. b) Time to failure of concrete elements under creep load in uni-axial tension [6].

* Corresponding author. Tel.: +27 21 808 4498; fax: +27 21 808 4947.
E-mail address: bboshoff@sun.ac.za (W.P. Boshoff).

0008-8846/$ - see front matter
doi:10.1016/j.cemconres.2007.02.001

Table 1
Mix proportions for the chosen SHCC mix

	Mass kg/m^3
Water	423
Cement	423
Fly ash	528
Slag	106
Fine sand	528
Super plastizer	10.6
Viscous agent	3.17
PVARecs 13	26.0

method is commonly used whereby the time-dependant strain of a cement-based material under a sustained load is divided into three components, namely drying shrinkage, basic creep and drying creep. Drying shrinkage is the length change of an unsealed and unrestrained specimen in a climate controlled environment and basic creep is the length change of a sealed specimen under a constant load. Drying creep is the increased creep found when a specimen is loaded and allowed to dry as the combination of the drying shrinkage and the basic creep measurements are less than the total measured length changed. This apparent mechanism was first pointed out by [11] and can attributed to surface cracking of the shrinkage specimen [11,12] and stress-dependant shrinkage occurring in the unsealed creep specimen [13].

In Fibre Reinforced Cement-based Composites (FRCC) the same time-dependant mechanisms act, while more are introduced in terms of fibres and the fibre-matrix interaction. Experimental studies on FRCC report conflicting findings on the effect of the fibres on creep and shrinkage. It has been reported [14,15] that steel fibres are effective in reducing creep in concrete. However, in contrast [16,17] reported that the creep strains of concrete specimens reinforced with small amounts of steel and polypropylene fibres are consistently higher than that of specimens without fibres.

This paper focuses on the time-dependant behaviour of a special class of FRCC, namely SHCC (Strain-Hardening Cement-based Composites), often referred to as ECC (Engineered Cement-based Composites). SHCC was engineered to overcome the weaknesses of ordinary concrete, which is a low tensile strength, brittleness and large cracks that have durability impairing implications. SHCC shows high ductility as it can resist the full tensile load at a strain of more than 3%. This superior response is achieved with multiple cracking under tensile loading which has a pseudo strain-hardening phenomenon as a result. The reader is referred to [18] for an in depth discussion of SHCC.

Table 2
Test program for the tensile rate tests with the normal testing rate emphasised

Number of specimens	6	6	9	5	5
Loading rate [/s]	10.4 μ	**104 μ**	1040 μ	0.0104	0.104

In order to appropriately apply SHCC in the construction industry, it is essential to understand and characterise its long-term behaviour. Limited results of some types of SHCC have been published [19–21] but no results are available of the tensile creep of SHCC. This inspired the research project to both characterise and model the time-dependant behaviour of ECC. To identify the added sources of the time-dependant behaviour of SHCC, rate and creep tests are envisaged on the meso-level (a level where the pull-out of a fibre is prominent) and the macro-level. A constitutive model for macroscopic finite element analysis of ECC has been developed and implemented recently [22] with the aim to simulate the time-dependant behaviour. As a first step in this ongoing research project, the experimental results of rate-dependant tensile and flexural tests are reported as well as the uni-axial tensile creep of SHCC specimens. The results of shrinkage tests of SHCC are also reported.

2. Experimental program

For this study of the time-dependant behaviour of SHCC, experimental tests were performed to determine the nature and identify the source of the time-dependant behaviour

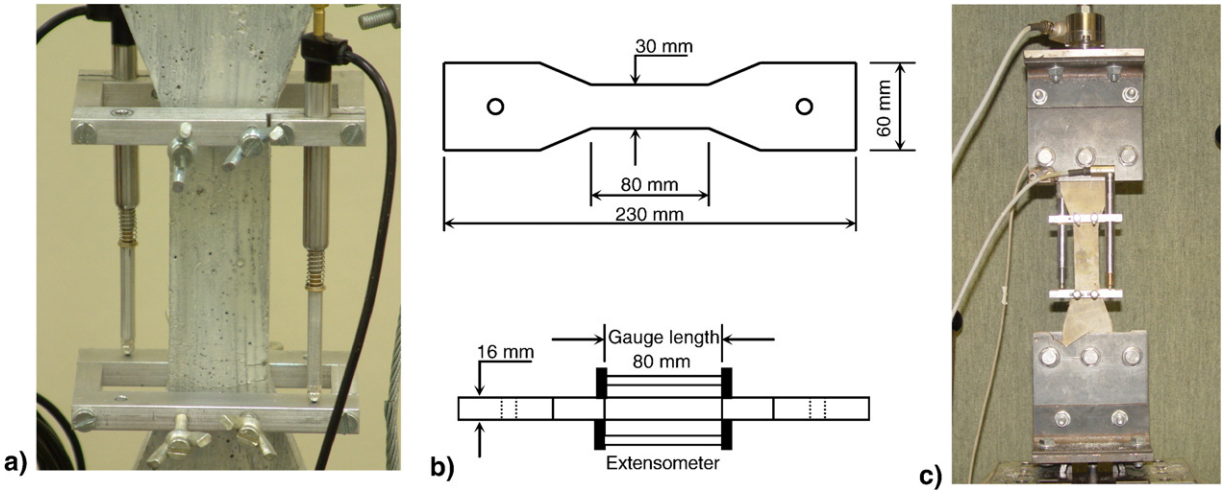

Fig. 2. a) The extensometer consisting of an aluminium frame and two LVDTs. b) The thin, flat shaped specimen. c) The tensile test setup in the Zwick Z250.

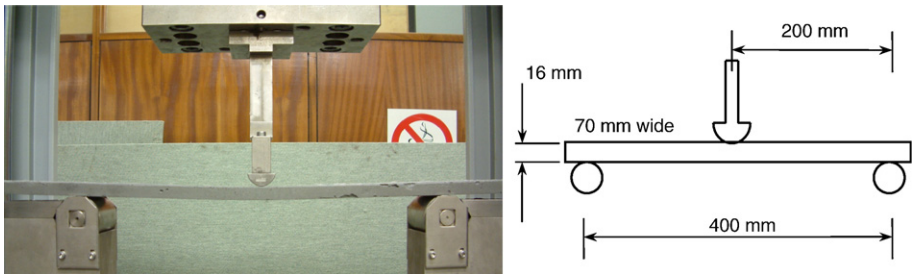

Fig. 3. Three point bending setup and the bending specimen.

as well as to quantify the tensile creep response. All tests were done using the same mix proportions, namely a water/binder ratio of 0.4 and an aggregate/binder ration of 0.5. The binder consisted of CEM I 42.5 cement, a fly ash filler marketed as PozzFill by Ash Resources, South Africa, and Corex Slag of origin of the Saldanha Steel Refinery in the Western Cape Province, South Africa used in the ratio of 45:50:5 by mass respectively. The mix proportions with the additives are given in Table 1. Note that the rheology refinement was achieved by the addition of a superplastizer and a viscosity modification agent.

The test specimens were cast in a steel mould while vibrated on a vibration table. The specimens were protected using steel plate covers and stripped three days after casting and further cured in water at 23 °C. All specimens were tested at an age of 14 days and were dried with a cloth just before testing. For the entire duration of the curing process as well as during the testing, the environment was kept constant at a temperature of 23 °C and the humidity was controlled at 65±5%.

Tensile rate tests were performed as well as rate tests of beams in three point flexure. The tensile rate tests represent the material on a macroscopic level while the flexural tests simulated the behaviour of SHCC in a more general structural sense as a strong strain gradient exists. Tensile creep tests were performed to characterise and quantify the tensile creep behaviour.

2.1. Tensile rate tests

The uni-axial tensile rate tests were done using a Zwick Z250 Universal Materials Testing Machine. The flat, thin specimens used are shown in Fig. 2 together with the clamps used to grip the specimens. The strain readings were taken by two HBM LVDTs, each with a range of 10 mm and attached to the specimens using a frame shown in Fig. 2, resulting in a gauge length of 80 mm. The force was measured with a HBM U2a 500 kg load cell. The test program is shown in Table 2.

2.2. Flexural rate tests

The flexural rate tests of SHCC beams were performed using the three point bending test setup of the Zwick Z250. The force and deflection were measured with the internal load cell and the crosshead displacement measuring device respectively. The test setup and the beam dimensions are shown in Fig. 3 and the test program is shown in Table 3.

2.3. Tensile creep tests

The tensile creep tests were performed using a method of applying the load with free hanging weights acting with a level arm on two specimens in series. The force acting on the specimens were calibrated by placing a HBM U2a 500 kg load cell in the position of the specimens to find the actual load corresponding to the applied weight. The setup can be seen in Fig. 4a). The strain of each specimen was measured with two LVDTs fixed to an aluminium frame as in the case for the tensile tests. To distinguish the creep strain from the time-dependant strain measured on the creep specimens, the drying shrinkage strain must be deducted. To measure the drying shrinkage strains, two specimens were allowed to dry with no axial constraint and the length change was measured over time.

3. Experimental results

3.1. Tensile rate tests

Five sets of tensile tests were done at different strain rates, covering four orders of magnitude. The responses are shown in Fig. 5.

An unexpected phenomenon was observed at the two high rates (0.0104/s and 0.104/s), i.e. a reduction of the stress after the first cracking point. This drop is common for ordinary FRCC, but not for SHCC. After the reduction, the expected strain-hardening occurs which is expected for SHCC. An explanation of the mechanism which causes this phenomenon is given in Section 4.1. As this first cracking strength could be higher than the stress at the onset of localising for the high strain rates, the ultimate strength of the material is defined as the highest stress reached after the load drop coinciding with the first cracking point.

The definition of the first cracking stress is shown in Fig. 6 for a high and low strain rate. The more classic definition would be to find the point where the response deviates substantially from the virgin elastic behaviour, but the proposed method is

Table 3
Test program for the flexural rate tests with the normal testing rate emphasised

Number of specimens	5	5	5	5	5
Loading rate [/s]	3.3 μm	8.3 μm	**83.3 μm**	0.83 mm	8.3 mm

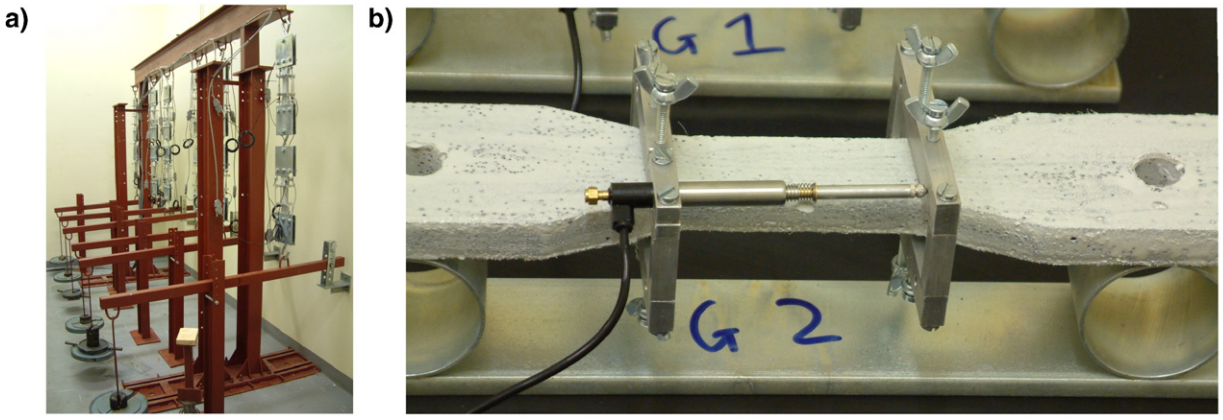

Fig. 4. a) Tensil creep setup. b) Shrinkage setup.

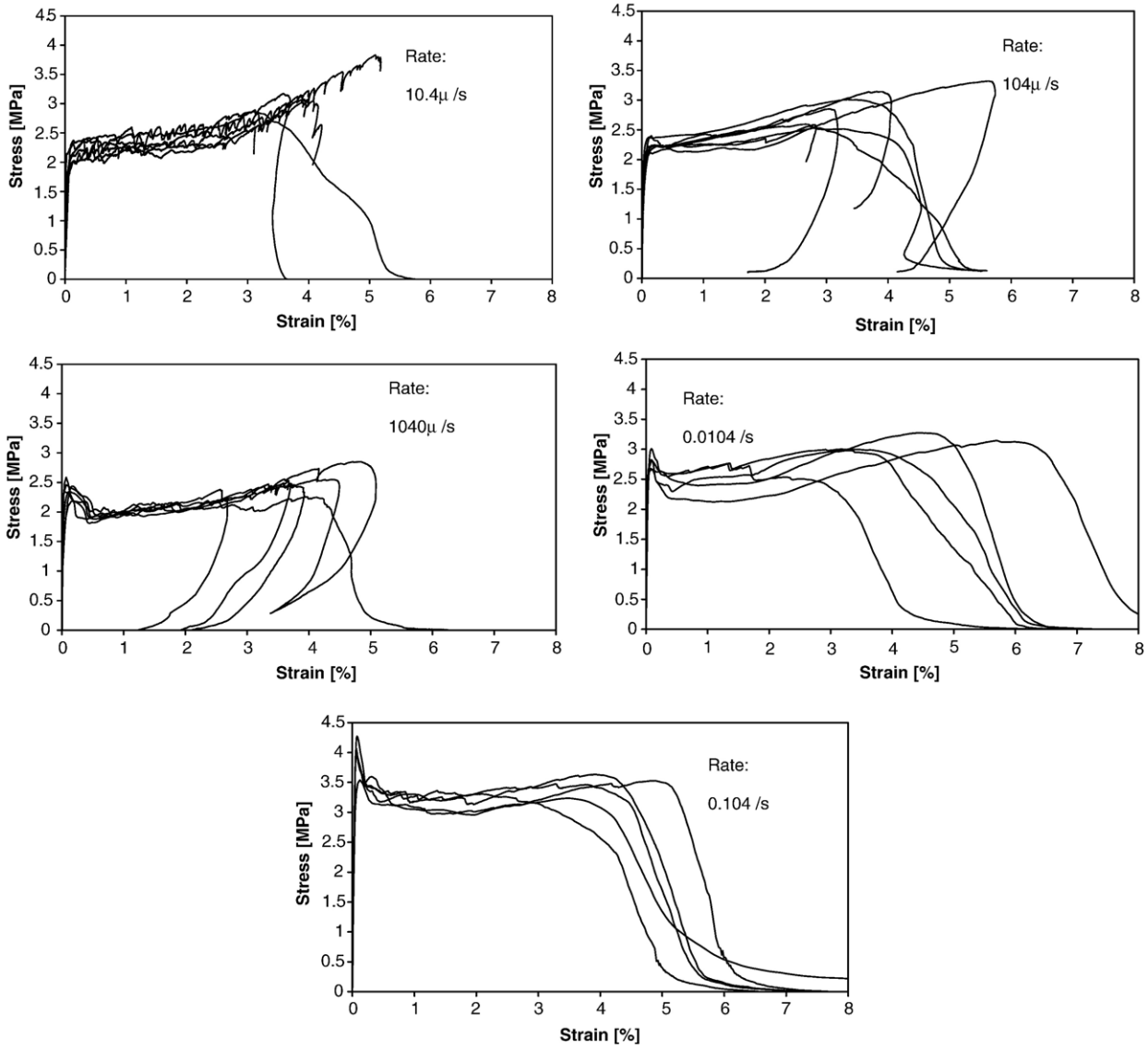

Fig. 5. The results of the tensile rate tests.

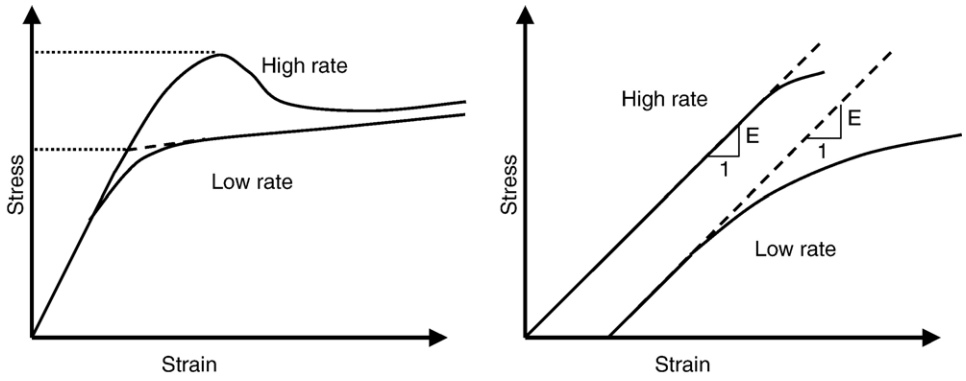

Fig. 6. The definition of the first cracking point (left) and the *E*-modulus (right) for low high rates.

more objective, especially if these results are to be used as parameters for a phenomological numerical model.

The definition of the *E*-modulus is difficult as the micro-cracking that causes the non-linear behaviour coincides with the fibres transferring the load. The non-linear behaviour is more prominent in the lower rates, which makes the objective determination of *E*-values a complex task. A pragmatic approach was used, namely to take the initial slope of the test results as shown in Fig. 6.

The average values as well as the minimum and maximum values of the first cracking stress, ultimate stress, ductility (which is defined as the strain at the point of the ultimate stress) as well as the *E*-modulus are shown in Fig. 7(a to d) for the different strain rates.

3.2. Flexural rate tests

The flexural rate tests were performed over a range of almost four orders of magnitude of the deflection rate. The responses are shown in Fig. 8. The average values as well as the minimum and maximum values of the first cracking force, ultimate force and the ductility are shown in Fig. 9. Note that the definitions of these values are the same as for the tensile results.

3.3. Tensile creep tests

The tensile creep and shrinkage tests were ended after 8 months of monitoring the response. The time-dependant responses of the individual shrinkage and creep specimens are

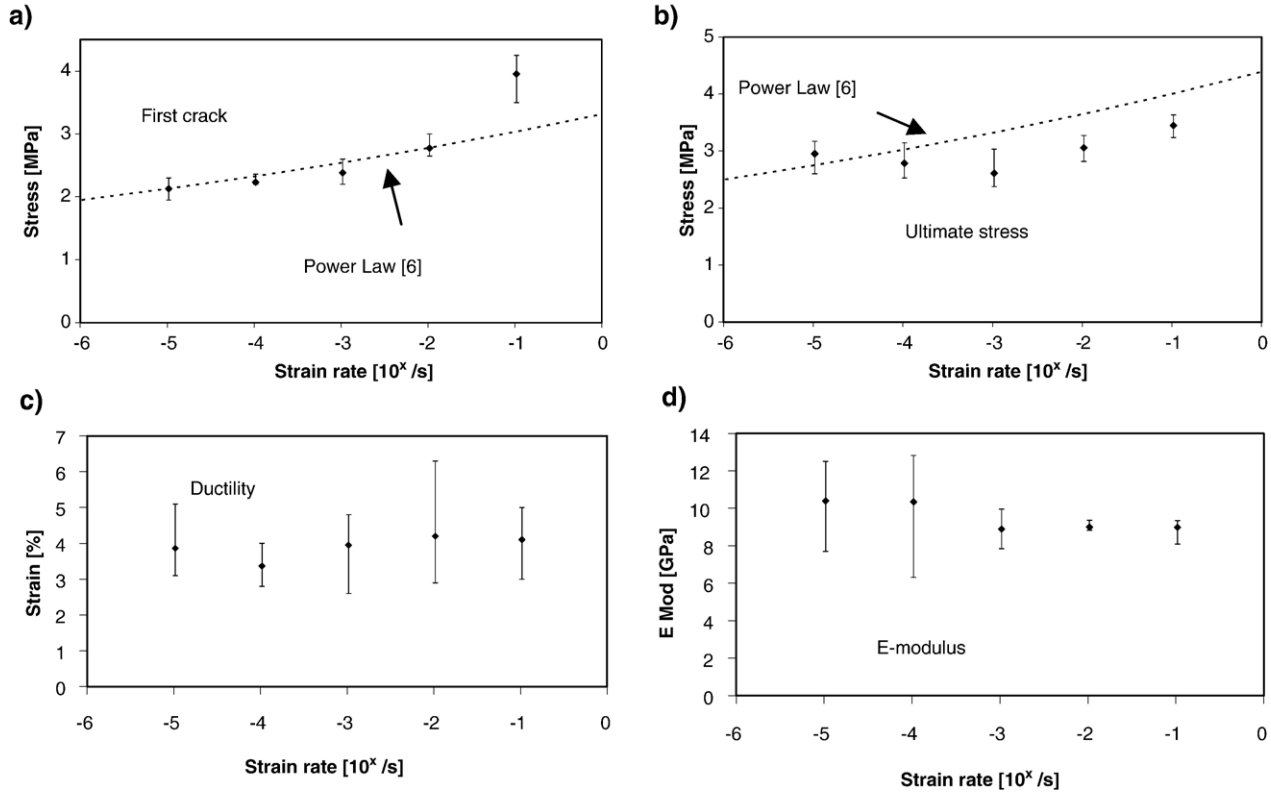

Fig. 7. Results of the tensile rate tests: a) first cracking stress, b) ultimate stress, c) ductility and d) *E*-modulus.

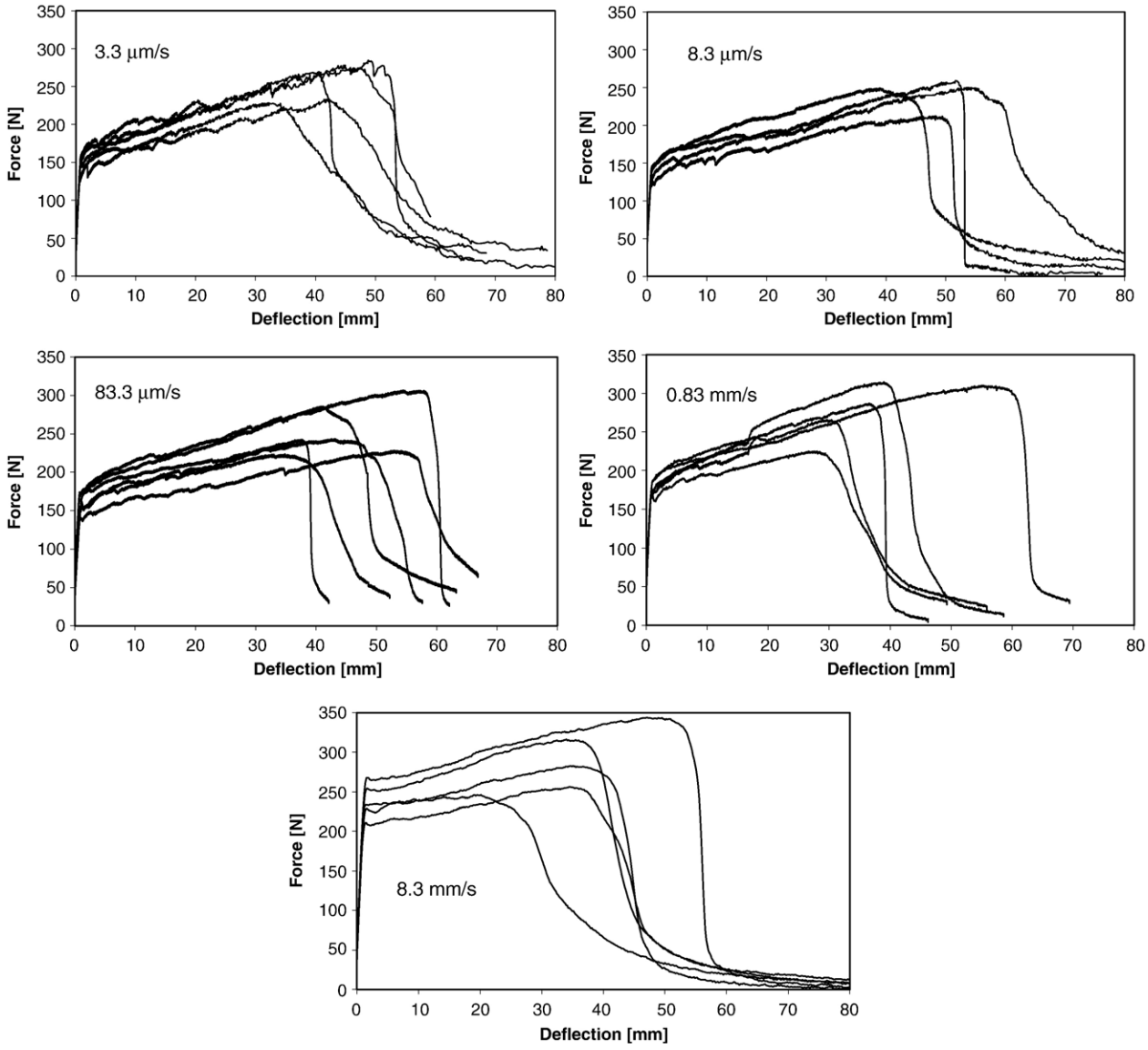

Fig. 8. The results of the deflection rate tests.

shown in Fig. 10. Tensile strain is denoted as positive. The instantaneous elastic portion of the strain which occurred during the application of the load is deducted in the case of the creep specimens. Note that about 4 h after load application, one of the loaded specimens showed a sudden increase of strain as shown in Fig. 11a. This was caused by a crack forming in the specimen, shown in Fig. 11b.

The Picket effect has been discussed briefly in the Introduction. As no sealed creep results are available, the basic and drying creep cannot be distinguished from each other. The total creep, i.e. the basic and drying creep together, can however be calculated by subtracting the drying shrinkage strain from the time-dependant response of the unsealed creep specimens. It is important to note that the result is not a true material parameter, as the drying creep, which is included in the total creep, is dependant on the geometry and rate of drying. The result would however give a good indication of the magnitude of the creep expected, especially if SHCC is used as a thin membrane member which the flat, thin specimen represents.

Due to the cracking during testing of the one creep specimen, only one specimen is available to represent the time-dependant response of the matrix under a sustained load. An envelope is shown of the calculated total creep in Fig. 12 using the results of the two shrinkage specimens and the tensile creep specimen that did not crack.

4. Discussion

4.1. Tensile rate tests

It is apparent from Fig. 5 that a typical ECC strain-hardening response was obtained for all specimens in direct tension, except for the drop in stress after the first crack in the high strain rate results. Moreover, reasonable repeatability was found, indicated by for instance a coefficient of variation of less than 10% in ultimate tensile strength of all rates.

The sudden decrease of stress after the first cracking is an unexpected phenomenon, especially in the direct tensile tests.

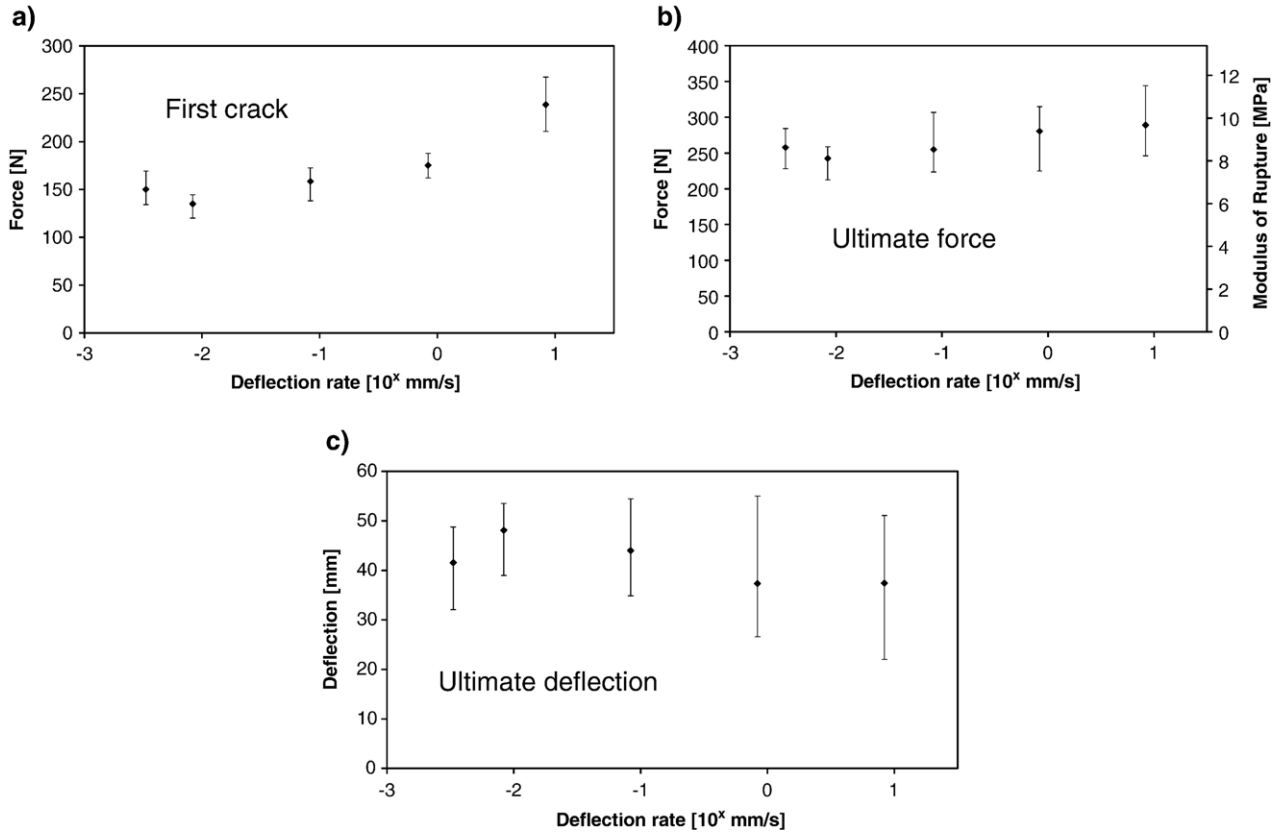

Fig. 9. Results of the flexural rate tests: a) fist cracking force, b) the ultimate force and c) the ultimate deflection.

This can however be explained if one considers the local strain rates at specific material points. It has been shown in this article and is also well-known that an increased loading rate increases the cracking resistance of a cement-based matrix. Before the point of first cracking, the strain rate can be considered approximately uniform throughout the material in a direct tensile test. At the point of cracking, the strain rate is increased almost infinitely at the crack plane due to the crack formation and opening, causing the strain rate over the rest of the material to decrease rapidly. Thus, the strain rate at the second crack position is much lower than the first crack point, resulting in a lower cracking stress.

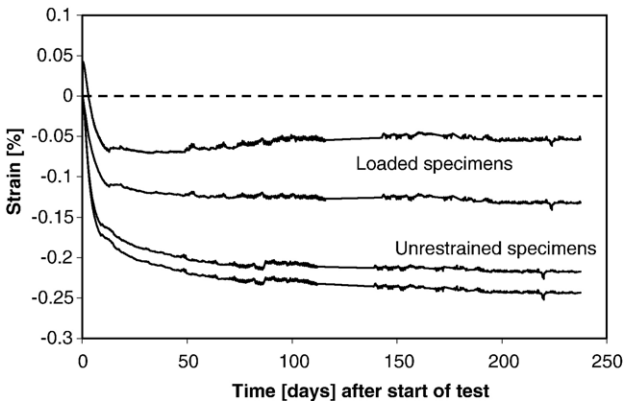

Fig. 10. Individual creep and shrinkage responses.

As mentioned in the Introduction, [6] used a power law to model the increase of the fracture stress of concrete with an increase of loading rate as follow:

$$\frac{\overline{\sigma}}{\overline{\sigma}_0} = \left(\frac{\dot{\sigma}}{\dot{\sigma}_0}\right)^{1/(\beta+1)} \tag{1}$$

with $\overline{\sigma}$ and $\dot{\sigma}$ the average stress and stress rate, $\overline{\sigma}_0$ and $\dot{\sigma}_0$ a reference stress and stress rate and β a material parameter.

This equation is plotted in Fig. 7 for the first cracking strength of SHCC as well as the ultimate strength. A typical value for compression of 25.0 is used for β [6] as no value is available for tensile behaviour. The lowest rate is used as a reference.

It is clear that the increase of the first cracking strength is what is expected of a cement-based material, except for the high rate nearing dynamic rate. However, for the ultimate stress the experimental increase of the stress with an increasing rate is less than expected for a cement-based material. However, the failure mechanism at the ultimate load is not the matrix failure as in the case of the first cracking strength, but the fibres bridging a crack either pulling out or rupturing. The source of the slight increase of the ultimate stress with an increase of rate would be found in the fibre or fibre–matrix interface and not the matrix.

The ductility and E-modulus was found to be insensitive to the increase of the loading rate. Note that the E-modulus was taken as the initial slope of the elastic portion of the tensile response. A secant E-modulus approach to a high proportionate load may have shown rate dependence.

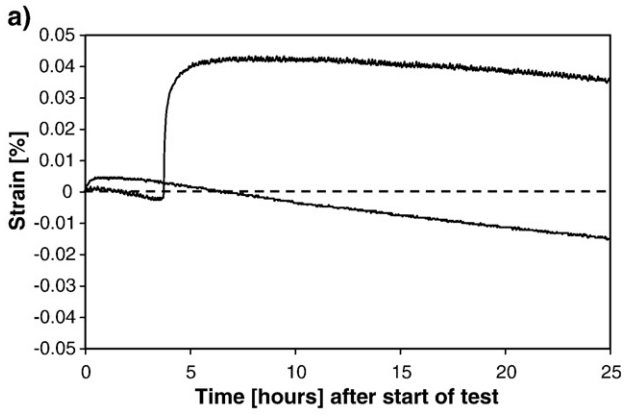

Fig. 11. a) A sudden increase of strain of the creep response. b) The crack that caused this increase.

4.2. Flexural rate tests

The power law model of [6] for the flexural first cracking strength increase with an increase of loading rate is shown in Fig. 13. A typical value of β for flexure of 18.0 was used [6]. The model predicts the increase of strength well, except once again for the highest deflection rate.

As for the tensile rate tests, only a slight increase of the ultimate strength was found with an increase of the deflection rate. The flexural ductility, unlike in the case of the tensile rate tests, did show a decrease with an increase of deflection rate.

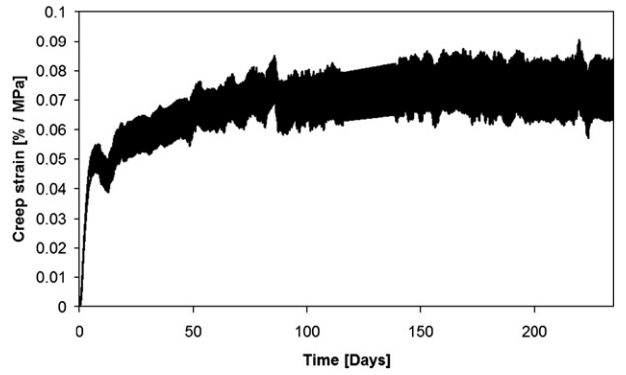

Fig. 12. The envelope for the total creep response.

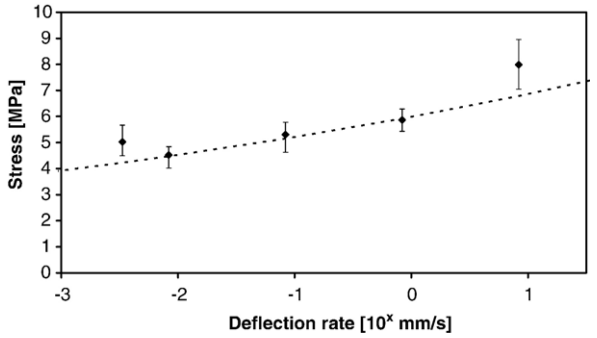

Fig. 13. The experimental results of the flexural first cracking stresses compared to the power law simulation.

This decrease is due to the increase of the first cracking strength of the material in tension. If the cracking strength of the material increases, the area that undergoes multiple cracking in flexure is decreased. This results in less flexural ductility. This implies that even if SHCC shows no reduction in ductility in tension with an increase of loading rate, a reduction could still occur in flexure.

4.3. Tensile creep tests

After 8 months of a sustained load as high as 50% of the ultimate load, the shrinkage still dominates the time-dependant response as seen in Fig. 10. The characterisation of the creep response is nevertheless important, as with different boundary conditions the creep response could become dominant. For example, if a beam is loaded in flexure while it is unconstraint in the axial direction, the shrinkage would have no effect on the deflections and the creep will increase the long-term deflections.

The creep envelope shown in Fig. 12 includes both the basic as well as the drying creep. It is important to note that due to the dependence of the drying creep on the specimen geometry, the values of creep are only valid for a geometries similar to the one used in the reported creep test.

It is common practice to relate creep responses to a creep compliance or a creep coefficient. The creep compliance factor, C_c is defined as the creep strain over a period of time per unit of stress as follows:

$$C_c = \frac{\varepsilon_c}{\sigma} \tag{2}$$

with C_c the creep compliance, ϵ_c the creep strain and σ the applied stress. The creep coefficient is defined as:

$$\Phi = \frac{\varepsilon_c}{\varepsilon_e} \tag{3}$$

with ϵ_e the elastic strain. It is useful to determine the long-term material stiffness, E_{long}, using:

$$E_{long} = \frac{E}{1+\Phi} \tag{4}$$

with E the elastic modulus at the time of loading.

Table 4
The creep results summarised

Creep compliance, C_c [mm/m/MPa]		Creep coefficient, Φ [–]	
8 months	30 years	8 months	30 years
0.68	0.98	6.3	9.0

It is commonly accepted that at 8 months, around 70% of the 30 year creep has occurred [23]. Taking this into account, the magnitude of creep is summarised in Table 4 using Eqs. (2) and (3).

The response of the shrinkage specimens is typical of a cement-based material. At the initial stage a large amount of shrinkage can be seen and the shrinkage rate reduces as time goes by. The shrinkage strain apparently stabilizes at an average strain of 0.23% after about 200 days of drying.

New important sources of tensile creep in SHCC are discovered in the creep specimen that cracked, namely a time-dependant crack formation and a possible increase of creep of a cracked specimen. It is shown that at a sustained load 50% of the ultimate static strength, crack initiation is possible which causes a sudden increase of creep. A second source of time dependence is seen in the creep rate of the two loaded specimens in Fig. 11. The cracked specimen shows a higher rate of creep compared to the uncracked specimen. Possible explanations of this increased creep are the creep of the fibres bridging the crack, the time-dependant fibre pull-out and/or the further time-dependant initiation of cracks which is not visible to the naked eye. Further investigation into the tensile creep behaviour is required to determine the true source of this time-dependant behaviour.

5. Conclusions

The importance of consideration of time dependence of the mechanical behaviour of cement-based composites has been argued. Experimental results of rate-dependant tests preformed in tension and flexure as well as the tensile creep response have been reported. The following conclusions can be drawn:

- The first cracking strength of SHCC in tension and in flexure increases with an increase of strain rate. It has been showed that the increase is in the same order as ordinary cement-based materials.
- The ultimate strength of the material in tension and flexure did not increase significantly with an increase of loading rate. This shows that the ultimate strength is less dependant on the loading rate than in ordinary concrete.
- The tensile ductility is independent of the loading rate for this type of SHCC. The flexural ductility did however decrease with an increase of the loading rate. This decrease is a result of the increase of the first cracking strength which causes a smaller area of multiple cracking in flexure with an increase of the loading rate.
- The tensile creep compliance was found to be 0.68 mm/m/MPa after 8 months loaded at half the static strength.
- The shrinkage behaviour of SHCC found is typical of a cement-based material. A drying shrinkage value of 0.23% was found for SHCC specimens tested in a controlled environment.
- A new source of time-dependant tensile strain has been identified: the time-dependant crack initiation under a sustained tensile load. This occurred at a load of 50% of the static tensile strength. The creep rate also increased after the crack initiation which indicates an increased creep rate under tension for cracked SHCC which could be caused either by fibre creep or time-dependant fibre pull-out.

Acknowledgements

The support of this research by the South African Cement and Concrete Institute, Infraset Infrastructure Products, as well as the Technology and Human Resources in Industry Programme of the South African Ministry of Trade and Industry is gratefully acknowledged. The supply of PVA fibres by Kuraray Co. Ltd. is appreciated.

References

[1] H. Rüsch, Researches toward a general flexural theory for structural concrete, ACI Journal 57 (1) (1960) 1–28.
[2] Z.P. Bažant, R. Gettu, Rate effects and load relaxation in static fracture of concrete, ACI Materials Journal 89 (5) (1992) 456–468.
[3] F.P. Zhou, Time-dependent crack growth and fracture in concrete, PhD thesis, (University of Lund, Sweden, 1992).
[4] Z.P. Bažant, Y. Xiang, Crack growth and lifetime of concrete under long time loading, Journal of Engineering Mechanics 123 (4) (1997) 350–358.
[5] G.P.A.G. Van Zijl, R. De Borst, J.G. Rots, The role of crack rate dependence in the long-term behaviour of cementitious materials, International Journal of Solids and Structures 38 (30–31) (2001) 5063–5079.
[6] H.A.W. Cornelissen, A.J.M. Siemes, Plain concrete under sustained tensile or tensile and compressive fatigue loadings, research on structural concrete 1982–1986, Report 25–87–66 Stevin Laboratory, Delft University of Technology, 1984, pp. 68–79.
[7] H. Mihashi, F.H. Wittmann, Stochastic approach to study the influence of rate of loading on strength of concrete, Heron 25 (3) (1980) 5–54.
[8] A.A. Griffith, The phenomena of rupture and flow in solids, Philosophical Transactions of the Royal Society of London. A 221 (1920).
[9] Z.P. Bažant, Mathematical Modelling of Creep and Shrinkage of Concrete, John Wiley and Sons, 1980.
[10] G.P.A.G. Van Zijl, R. De Borst, J.G. Rots, The role of crack rate dependence in the long-term behaviour of cementitious materials, International Journal of Solids and Structures 38 (2001) 5063–5079.
[11] G. Pickett, The effect of change in moisture content on the creep of concrete under a sustained load, ACI Journal 38 (1942) 333–355.
[12] F.G. Wittmann, P.E. Roelfstra, Total deformation of loaded drying concrete, Cement and Concrete Research 10 (1980) 601–610.
[13] Z.P. Bažant, Y. Xi, Drying creep of concrete: constitutive model and new experiments separating its mechanisms, Materials and Structures 27 (1994) 3–14.
[14] P.S. Mangat, M.M. Azari, Compression creep behaviour of steel fibre reinforced cement composites, Materiaux et Constructions 19 (113) (1986) 361–370.
[15] J.C. Chern, C.H. Young, Compressive creep and shrinkage of steel fibre reinforced concrete, International Journal of Cement Composites 11 (4) (1989) 205–214.
[16] P.N. Balaguru, V. Ramakrishnan, Properties of fiber reinforced concrete: workability, behavior under long-term loading, air-void characteristics, ACI Materials Journal 85 (3) (1988) 189–196.

[17] J. Houde, A. Prezeau, R. Roux, Creep of Concrete Containing Fibers and Silica Fume Fiber Reinforced Concrete Properties and Applications, ACI, Detroit, MI, 1987 (ACI SP-105).
[18] V.C. Li, From micromechanics to structural engineering. The design of cementitious composites for civil engineering applications, Journal of Structural Mechanics Earthquake Engineering, JSCE 10 (2) (1993) 37–48.
[19] M. Maalej, S.T. Quek, J. Zhang, Behaviour of hybrid-fibre engineered cemetitious composites subjected to dynamic tensile loading a projectile impact, Journal of Materials in Civil Engineering-ASCE (2005) 143–152.
[20] K.S. Douglas, S.L. Billington, Rate dependencies in high-performance fibre-reinforced cement-based composites for seismic application, Proceedings of HPFRCC Conference, 2005, Hawaii.
[21] E. Yang, V.C. Li, Rate dependence in engineered cementitious composites, Proceedings of HPFRCC Conference, 2005, Hawaii.
[22] W.P. Boshoff, G.P.A.G. Van Zijl, Numerical modelling of ECC, in: V.C. Li, et al., (Eds.), Proceedings 5th Fracture Mechanics of Concrete and Concrete Structures (FRAMCOS-V), Vail, USA, 2004, pp. 1037–1043.
[23] F.K. Kong, R.H. Evans, Reinforced and Prestressed Concrete, Spon Press, London, Great Britain, 1987.